Article

Journal of
Nanoscience and Nanotechnology
Vol. 15, 8577–8583, 2015
www.aspbs.com/jnn

Etch Properties of Amorphous Carbon Material Using RF Pulsing in the $O_2/N_2/CHF_3$ Plasma

Min Hwan Jeon[1,†], Jin Woo Park[2,†], Deok Hyun Yun[2], Kyong Nam Kim[2], and Geun Young Yeom[1,2,*]

[1] *SKKU Advanced Institute of Nano Technology (SAINT), Sungkyunkwan University, Suwon, Gyeonggi-do 440-746, South Korea*
[2] *Department of Materials Science and Engineering, Sungkyunkwan University, Suwon, Gyeonggi-do 440-746, South Korea*

The amorphous carbon layer (ACL), used as the hardmask for the etching of nanoscale semiconductor materials, was etched using O_2/CHF_3 in addition to O_2/N_2 using pulsed dual-frequency capacitively coupled plasmas, and the effects of source power pulsing for different gas combinations on the characteristics of the plasmas and ACL etching were investigated. As the etch mask for ACL, a patterned SiON layer was used. The etch rates of ACL were decreased with the decrease of pulse duty percentage for both O_2/N_2 and O_2/CHF_3 due to decrease of the reactive radicals, such as F and O, with decreasing pulse duty percentage. In addition, at the same pulse duty percentage, the etch selectivity of ACL/SiON with O_2/CHF_3 was also significantly lower than that with O_2/N_2. However, the etch profiles of ACL with O_2/CHF_3 was more anisotropic and the etch profiles were further improved with decreasing the pulse duty percentage than those of ACL with O_2/N_2. The improved anisotropic etch profiles of ACL with decreasing pulse duty percentage for O_2/CHF_3 were believed to be related to the formation of a more effective passivation layer, such as a thick fluorocarbon layer, on the sidewall of the ACL during the etching with O_2/CHF_3, compared to the weak C–N passivation layer formed on the sidewall of ACL when using O_2/N_2.

Keywords: Pulsed Plasma, Etch Characteristics, Amorphous Carbon Material, DF-CCPs.

1. INTRODUCTION

For the patterning of nanometer scale semiconductor devices, shorter wavelengths of the light source for the photolithography from 193 nm ArF excimer laser to 13.56 nm extreme ultraviolet (EUV) are investigated to increase the resolution of photolithographic process.[1–5] The use of shorter wavelengths of the light source also tends to decrease the thickness and the stiffness of the photoresist due to lower depth of focus at shorter wavelengths. Therefore, critical problems such as pattern collapse and distortion, low etch selectivity, etc. are observed during the plasma etching, especially for the high aspect ratio contact etching. Therefore, as the etch mask for the nanometer scale device processing, hard mask materials composed of a multi-layer resist structure are used as the etch mask for the processing of devices on a nanometer scale to increase the etch selectivity between the etch mask and the materials to be etched, such as contact SiO_2, due to the difficulty in etching the materials directly using a single layer photoresist only.[6–8]

Among the various hard mask materials, amorphous carbon layer (ACL) has been widely used due to the high etch selectivity over a photoresist and Si-based materials, easy deposition, and easy removal after the dry etch process.[9–12] However, the etching of ACL using conventional oxygen chemistry tends to show non-ideal etch profiles such as bowing, necking, taping, and increased top/bottom open CD ratio.[13] Therefore, various additive gases such as N_2, H_2, HBr, etc. have been added to oxygen to improve the etched ACL profile by the passivation of the sidewall.[14–17] However, as the pattern size is decreased further down to tens of nanometers, the effect of those additive gases was not sufficient to maintain the anisotropic etch characteristics of ACL using the conventional oxygen-based plasma for sidewall passivation, due to a thin passivation layer remaining during the etching.

Recently, pulsed plasma techniques have been widely investigated for the highly selective etching of dielectric materials. By using rf pulsing, that is, by turning on and off

*Author to whom correspondence should be addressed.
†These two authors contributed equally to this work.

the rf power periodically at a certain frequency during the etching, several advantages have been reported, including improvement of the etch characteristics and reduction of the plasma-induced damage due to more effective control of the gas dissociation and ion bombardment energy.[18–21] The pulsed plasma is one of the most promising candidates for the control of radical ratios in the plasma. It is believed that the ACL etch profile can be also improved by using pulsed plasmas by the formation of effective passivation layer on the sidewall.

In this study, the effect of the pulsed plasma technique has been investigated in the etching the ACL layer using a dual-frequency capacitive coupled (DF-CCP) oxygen-based plasma and, in addition to the rf plasma pulsing, the effect of different gases to O_2, including N_2 and CHF_3, on the ACL etch characteristics, which can result in the formation of a passivation layer on the ACL surface during the etching for the anisotropic etching, was also examined. Therefore, in this study, the effect of pulsing for different gas additives on the etching characteristics of ACL was investigated in the 60/2 MHz DF-CCP.

2. EXPERIMENTAL DETAILS

The 60/2 MHz pulsed DF-CCP system used in this study is shown in Figure 1. The rf discharge was maintained between two parallel plate electrodes separated by 30 mm. The top electrode was covered with a perforated silicon plate to flow the reactive gases uniformly and it was connected to a 60 MHz rf power (HF) source which can be pulsed to control the plasma characteristics. The 60 MHz rf power was pulsed at 1 kHz of pulse frequency with the duty percentage from 100% (continuous wave: CW) to 25%. A continuous wave 2 MHz rf power was applied to the substrate while keeping the same average bias voltage. The reactor was evacuated by a turbo molecular pumps (3200 l/s) backed by a dry pump. The gas was equally distributed through a baffle system from the top electrode.

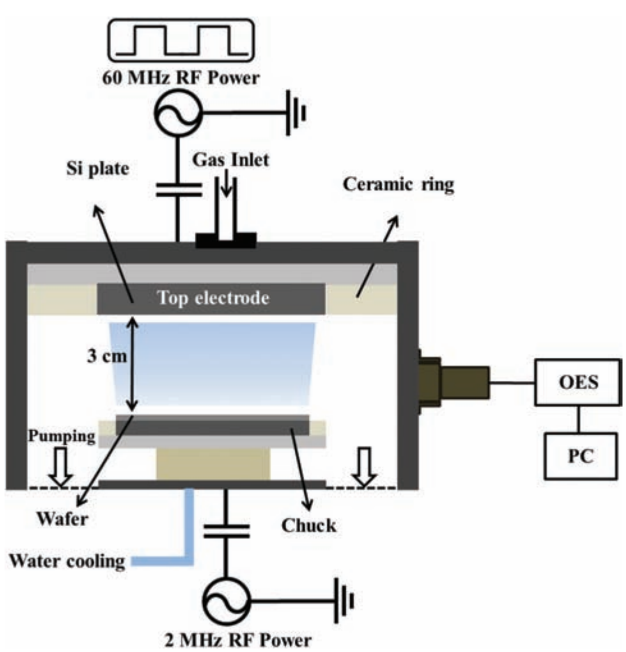

Figure 1. The 60/2 MHz pulsed DF-CCP system used in this study. The 60 MHz rf power was pulsed at 1 kHz of pulse frequency with the duty percentage from 100% (continuous wave: CW) to 25%. A continuous wave 2 MHz rf power was applied to the substrate while keeping the same average bias voltage.

The 600 nm thick ACL deposited on SiO_2 wafers was masked with 70 nm thick SiON layer as the etch mask for ACL. (A very thin photoresist layer used for the pattering SiON layer is remained on the SiON layer, however, it is completely removed during the initial etch period of ACL etching and the SiON layer is exposed.) The etch characteristics of the ACL were investigated using O_2/N_2 (40/60 sccm) mixture and O_2/CHF_3 (40/60 sccm) mixture in the 60 MHz source power/2 MHz bias power at 200 W/−300 V and the operating pressure of 20 mTorr while keeping the substrate temperature at room temperature. The optimized gas mixture ratios of O_2/N_2 and O_2/CHF_3 used in the experiment were determined by preliminary experiments at a CW source power condition.

The reactive radicals such as O, F, CF_2, etc. generated in the rf pulsed plasmas were studied using optical emission spectroscopy (OES, Andor iStar 734). The chemical binding characteristics on the etched ACL surface were observed with an X-ray photoelectron spectroscope (XPS, VG Microtech Inc., ESCA2000) using a Mg Kα twin-anode source, and the surface roughness of the etched ACL was analyzed with a high-resolution atomic force microscopy (HR AFM, INOVA). The profiles of the etched ACL patterns were observed by field emission scanning electron microscopy (FE-SEM, Hitachi S-4700).

3. RESULTS AND DISCUSSION

The effects of rf source power pulsing on the etch rates of ACL and SiON, and the etch selectivities of ACL/SiON were investigated for the gas mixtures of O_2/N_2 (40/60 sccm) and O_2/CHF_3 (40/60 sccm), and the results are shown in Figures 2(a) and (b), respectively. As the etch conditions, 200 W of 60 MHz source power and −300 V of 2 MHz bias voltage were used at the 20 mTorr of operating pressure. The pulse frequency of the 60 MHz source power was fixed at 1 kHz, and the pulse duty percentage was varied from 100% (CW) to 25%. As shown in Figure 2(a), the etch rates of ACL for O_2/N_2 and O_2/CHF_3 were generally decreased with decreasing the pulse duty percentage, except for the etching of SiON with O_2/N_2. In the case of etching of SiON with O_2/N_2, the change of etch rate with decreasing the pulse duty percentage was negligible because SiON does not form volatile etch products with radicals formed with O_2/N_2. When the etch selectivities of ACL/SiON were measured, as shown in

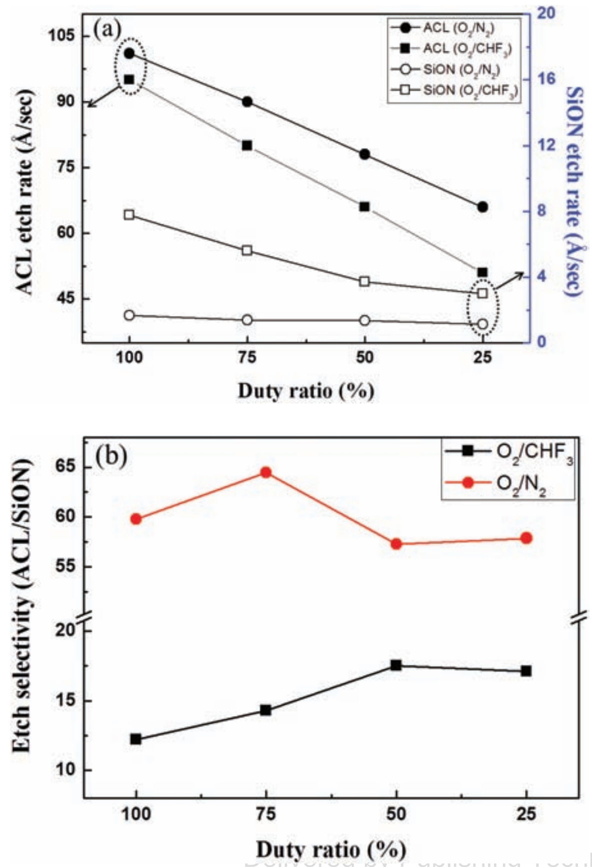

Figure 2. Effects of rf source power pulsing on (a) the etch rates of ACL and SiON, and (b) the etch selectivities of ACL/SiON for the gas mixtures of O_2/N_2 (40/60 sccm) and O_2/CHF_3 (40/60 sccm).

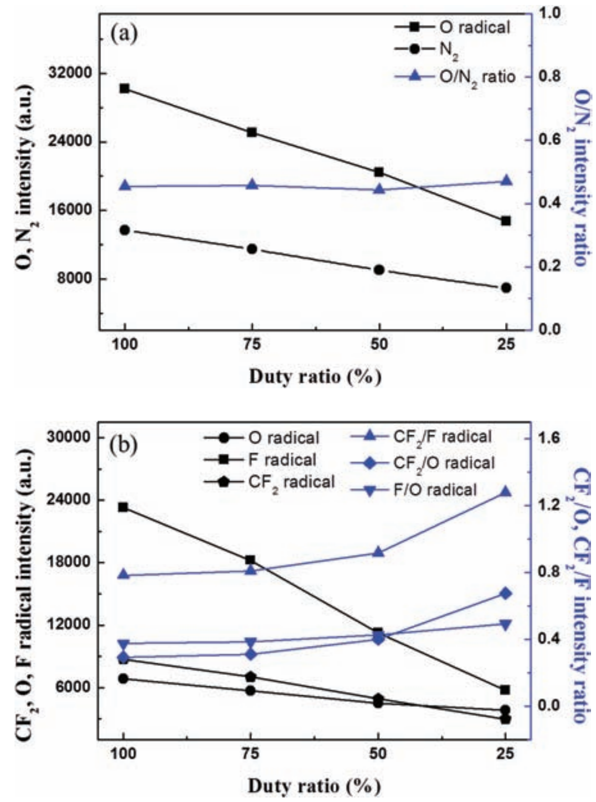

Figure 3. Change of the radical intensities in (a) O_2/N_2 plasmas and (b) O_2/CHF_3 plasmas measured using OES as a function of pulse duty.

Figure 2(b), the etch selectivity of the ACL/SiON for O_2/N_2 was slightly decreased with the decrease of duty percentage while that for O_2/CHF_3 was increased with decrease of the duty percentage, though the etch selectivities for O_2/N_2 were significantly higher than those for O_2/CHF_3.

The change of the radical intensities in the O_2/N_2 plasmas and O_2/CHF_3 plasmas were measured using OES as a function of pulse duty percentage, and the results are shown in Figures 3(a) and (b), for O_2/N_2 plasmas and O_2/CHF_3 plasmas, respectively. The plasma conditions were the same as those in Figure 2. The OES peak intensities for O, F, and CF_2 were measured at 777 nm, 703 nm, and 235∼255 nm, respectively. In the case of N, it is known to be difficult to be measured due to the significantly low intensity. Instead, a few peaks related to N_2 excited states were measured between 300∼400 nm; therefore, in our experiment, the OES peak intensity at 337 nm was used as the N_2 excited intensity. As shown in Figure 3(a), in the O_2/N_2 plasma, the optical peak intensities of the O and N_2 excited states were decreased with decrease of the pulse duty percentage; however, when the optical peak intensity of O/N_2 was measured, the ratio was remained similar regardless of the pulse duty percentage. Therefore, it appears to show that the O atomic density remains similar during the pulse-on time regardless of the pulse duty percentage, even though the average O atomic density is decreased with decreasing pulse duty percentage. In Figure 3(b), the optical emission peak intensities of O, F, and CF_2 and their ratios, CF_2/F, CF_2/O, and F/O, are shown. As shown in the figure, the decrease of pulse duty percentage decreased optical emission intensities of O, F, and CF_2; however, with decreasing the pulse duty percentage, the ratios of CF_2/F and CF_2/O were increased, while the F/O ratio was remaining similar. The increased ratios of CF_2/F and CF_2/O with decreasing pulse duty percentage are believed to be related to the increased radical recombination due to the increased pulse-off time in the pulse cycle. The decreased etch rates of ACL for O_2/N_2 and O_2/CHF_3, and the decreased etch rates of SiON for O_2/CHF_3 with decrease of the pulse duty percentage in Figure 2 are related to the decreased reactive species, such as O and/or F, in the plasma, as shown in Figures 3(a) and (b), which are required for the etching of ACL in addition to the increased CF_x formation for O_2/CHF_3 plasma.

The chemical binding states of the ACL surfaces etched with O_2/N_2 and O_2/CHF_3 were investigated with XPS to study the possible passivation layer formed on the ACL surface and the sidewall during the etching and the results are shown in Figures 4 and 5, respectively. Before the

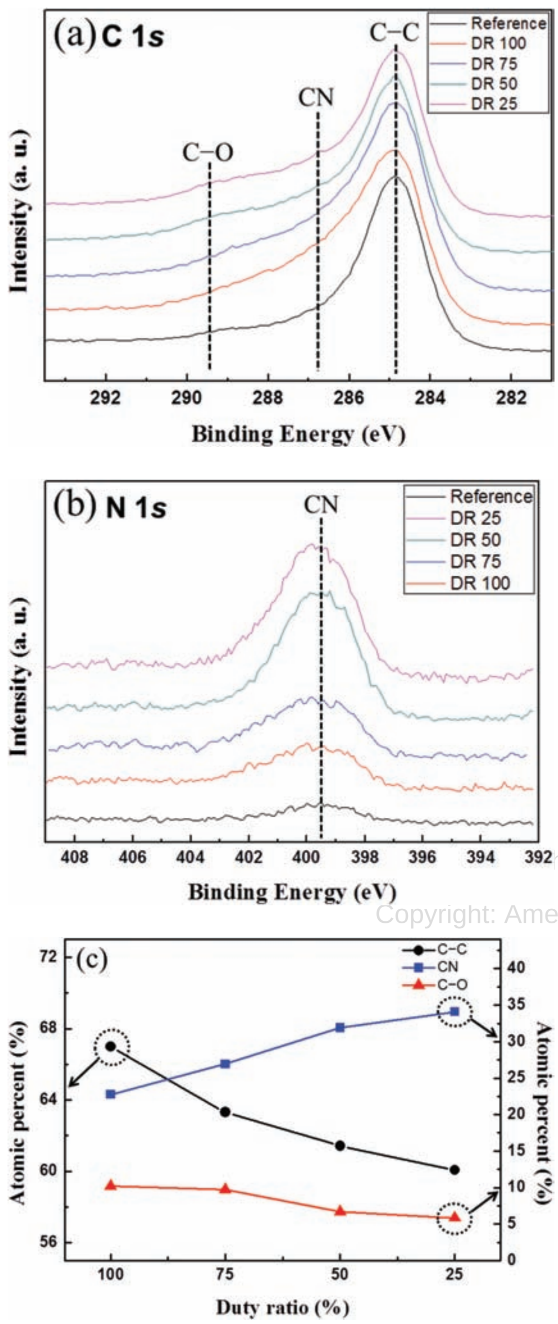

Figure 4. XPS narrow scan data of (a) C1*s* and (b) N1*s* of the ACL surfaces etched with O_2/N_2, and (c) relative percentages of the different carbon binding states such as C–C, CN, and C–O deconvoluted from (a).

XPS analysis, the ACL samples were etched with the same conditions shown in Figure 2 while varying the etching time to etch 600 nm thick ACL for both O_2/N_2 and O_2/CHF_3. In Figures 4(a) and (b), narrow scan data of C1*s* and N1*s* are shown. As shown in Figure 4(a), with decreasing the pulse duty percentage, the broadening of the C1*s* peak was observed and, in addition to the binding peaks related to C–C (284.8 eV), CN (287.8 eV; C–N and C═N) and C–O (289.5 eV) could be observed. Also, as shown in Figure 4(b), with decreasing the pulse duty percentage, the increase of the N peak intensity at 399.4 eV possibly related to the CN bonding on the etched ACL surface was observed. When the relative percentages of the different carbon binding states, such as C–C, CN, and C–O, deconvoluted from Figure 4(a) were measured, as shown in Figure 4(c), the increase of CN bonding on the ACL surface was observed with decreasing pulse duty percentage possibly indicating the formation of a CN passivating

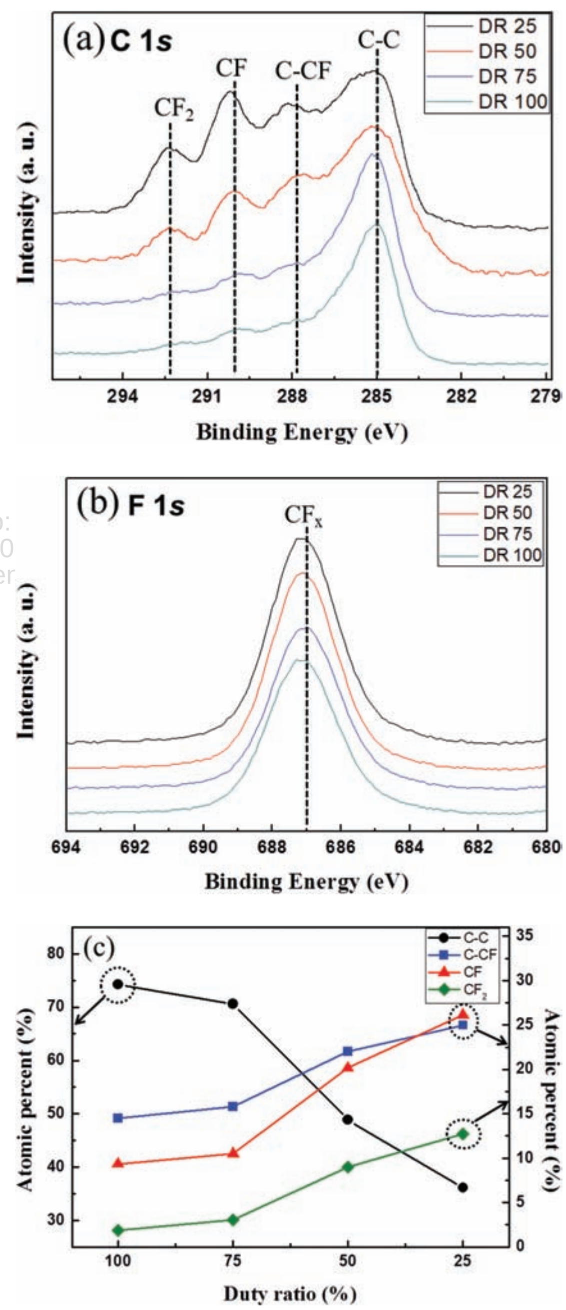

Figure 5. XPS narrow scan data of (a) C1*s* and (b) F1*s* of the ACL surfaces etched with O_2/CHF_3, and (c) relative percentages of the different carbon binding states such as C–C, C–CF, CF and CF_2 deconvoluted from (a).

layer on the ACL surface and sidewall during the ACL pattern etching.

The chemical binding states of the ACL surfaces etched with O_2/CHF_3 are shown in Figures 5(a) and (b) for C1*s* and F1*s*, respectively. The chemical binding peaks related to C–C (285 eV), C–CF (287.9 eV), CF (290.1 eV), and CF_2 (292.3 eV) were observed for C1*s*, in Figure 5(a) and the chemical binding state of F1*s* at 687.0 eV, possibly related to C–F_x ($x = 1\sim3$), was also observed for F1*s* in Figure 5(b) on the ACL surface etched with O_2/CHF_3. Also, the relative percentages of the carbon binding states are shown in Figure 5(c). As shown in Figure 5(c), with decreasing the pulse duty percentage, significant increases of C–CF, CF, and CF_2, indicating the thick fluorocarbon polymer passivation layer on the ACL surface could be observed possibly due to the increased CF_x/F and CF_x/O in the plasma with decreasing pulse duty percentage, as shown in Figure 3(b). The increased ratios of CF_x/F and CF_x/O in the plasma increase the fluorocarbon polymer deposition thickness on the ACL surface and sidewall during the ACL pattern etching at the decreased pulse duty percentage.

The surface roughness of the ACL after etching with O_2/N_2 and O_2/CHF_3 was also measured using AFM as a function of pulse duty percentage and the results are shown in Figure 6. For the AFM measurements, the ACL samples were etched about 600 nm with the conditions shown in Figure 2. As shown in the figures, the RMS surface roughness of ACL was the highest for the CW condition, and the decrease of the pulse duty percentage decreased the surface roughness. When the ACL samples etched using O_2/N_2 were compared with those etched with O_2/CHF_3, those etched with O_2/CHF_3 showed slightly lower RMS surface roughness compared to those etched with O_2/N_2 at the same pulse duty percentage. The decreased surface roughness with decreasing pulse duty percentage is believed to be related to the more uniform surface passivation layer formed on the ACL surface during the pulse-off time. The differences in the RMS surface roughness between the O_2/N_2 and O_2/CHF_3 may be related to the differences in the passivation layer characteristics formed on ACL the surface.

Figures 7 and 8 show the etch profiles of ACL etched with O_2/N_2 and O_2/CHF_3, respectively, for the different pulse duty percentages of (a) 100%, (b) 75%, (c) 50%, and (d) 25%. The etching conditions were the same as those used in Figure 2. About 600 nm thick ACL was etched and the ACL was masked with a 70 nm thick SiON mask. As shown in Figure 7, a slight improvement of the ACL etch profile was observed with decreasing duty percentage while not changing the thickness of the SiON mask. The improvement of the ACL etch profile was related to the formation of a C–N passivation layer on the sidewall of the ACL during the etching with decreasing pulse duty

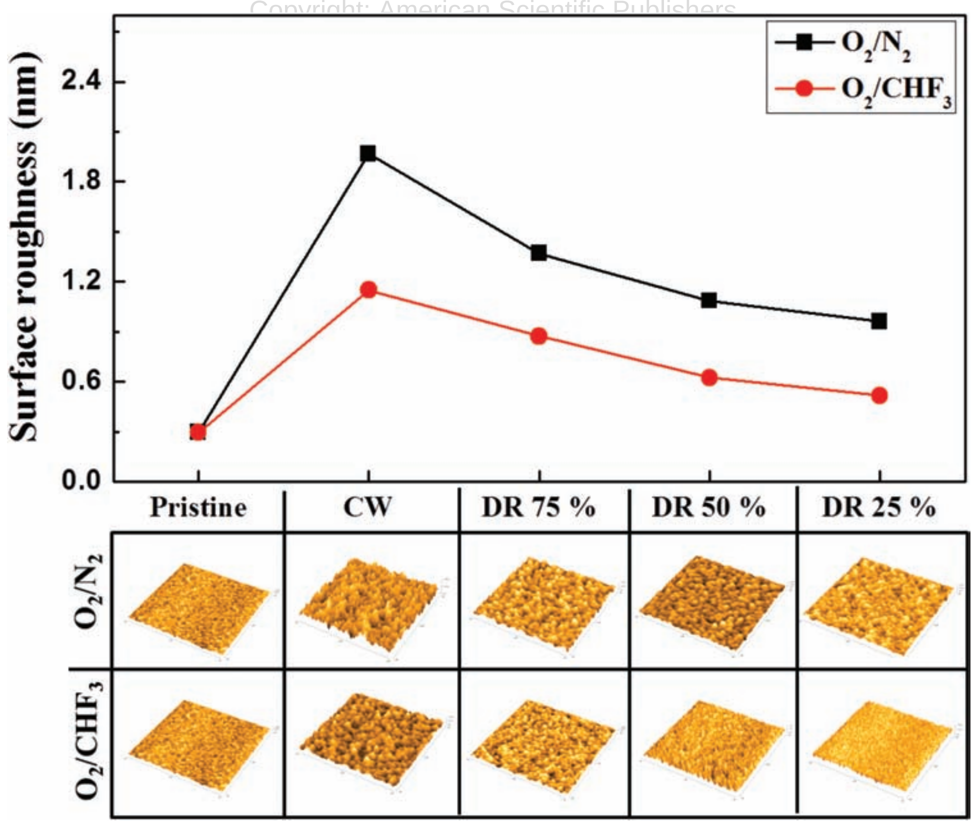

Figure 6. Surface roughness of the ACL after etching with O_2/N_2 and O_2/CHF_3, measured using AFM as a function of pulse duty percentage.

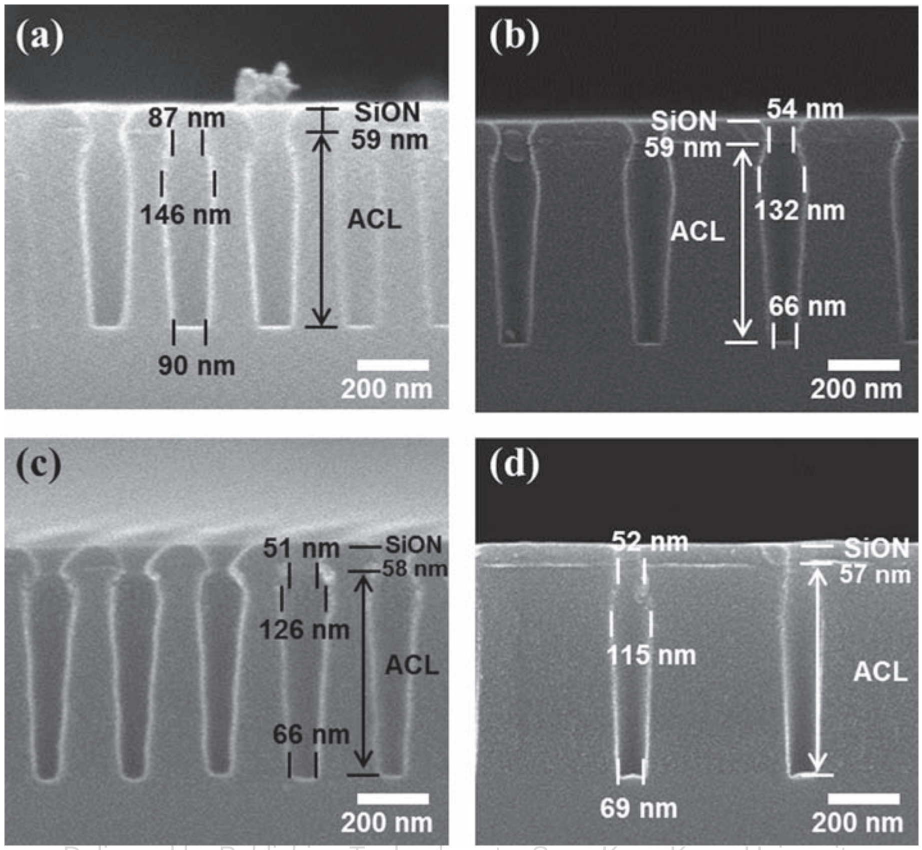

Figure 7. Etch profiles of 600 nm thick ACL masked with SiON etched with O_2/N_2 at different pulse duty percentages of (a) 100%, (b) 75%, (c) 50%, and (d) 25%.

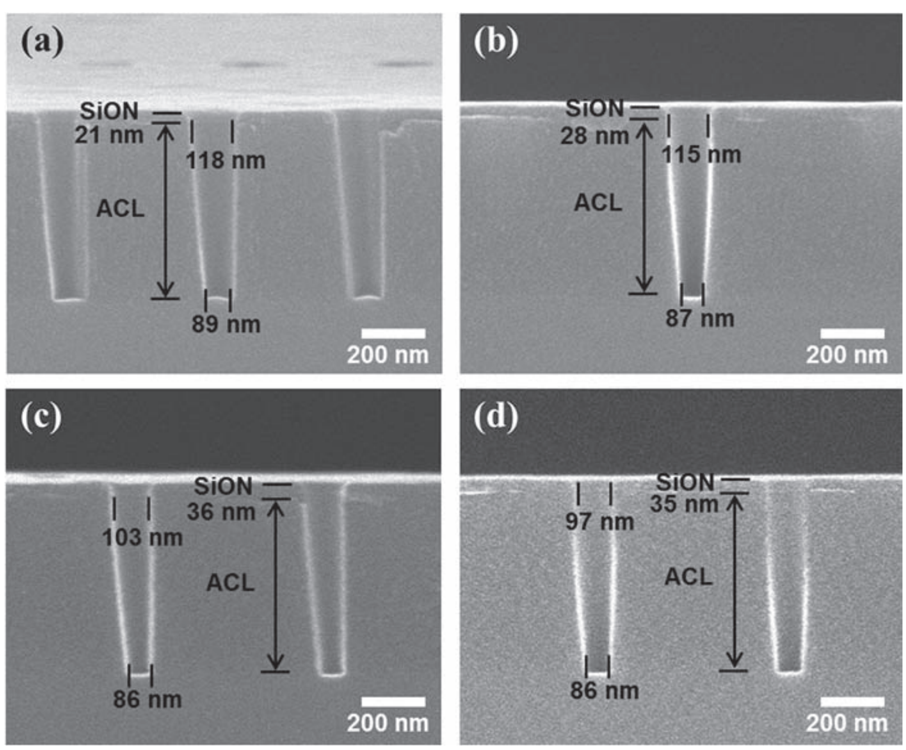

Figure 8. Etch profiles of 600 nm thick ACL masked with SiON etched with O_2/CHF_3 at different pulse duty percentages of (a) 100%, (b) 75%, (c) 50%, and (d) 25%.

percentage, as shown in Figure 4. However, as shown in Figure 7, sidewall necking and bowing of the etch profile was observed even after 25% pulse duty percentage possibly due to a thin/weak CN passivation layer formed on the sidewall, caused by the small change in the gas dissociation characteristics as a function of the pulse duty percentage for O_2/N_2.

When O_2/CHF_3 was used instead of O_2/N_2, as shown in Figure 8, the remaining SiON thickness was thinner for all of the pulse duty percentages compared to the SiON thickness observed for O_2/N_2 in Figure 7 due to the low etch selectivity of ACL/SiON. However, the etch profiles of ACL were more anisotropic, and the open critical dimension size was decreased with decreasing pulse duty percentage. The improved etch profile with decreasing pulse duty percentage was related to the more CF_x radicals to the surface and the thicker C–F polymer formed on the sidewall surface of the etched ACL, caused by the significant change in the ratios of gas dissociation species such as CF_x/O and CF_x/F as a function of the pulse duty percentage.

4. CONCLUSIONS

The ACL was etched using O_2/CHF_3 and O_2/N_2 in source power pulsed dual-frequency capacitively coupled plasmas and the effects on the ACL etch characteristic were investigated as a function of the source power pulse duty percentage. The ACL etch rates and etch selectivities of ACL/SiON with O_2/CHF_3 were lower than those with O_2/N_2. In addition, the ACL etch rates with O_2/CHF_3 were further decreased than those with O_2/N_2 with decreasing the pulse duty percentage. However, the etch profiles obtained with O_2/CHF_3 were more anisotropic compared to those obtained with O_2/N_2, and more improved etch profiles could be observed with decreasing pulse duty percentage. The more improvement of the anisotropic etch profiles of ACL with decreasing pulse duty percentage for O_2/CHF_3 was believed to be related to the formation of a more effective passivation layer on the sidewall of ACL during the etching with O_2/CHF_3 through the significantly different gas dissociation characteristics, which affected the passivation layer characteristics by the pulsing. Therefore, it is believed that pulsing should be applied to a certain gas combination such as O_2/CHF_3, rather than O_2/N_2, which can significantly change the dissociated radicals affecting the etching by pulsing.

Acknowledgments: This work was supported by the Industrial Strategic Technology Development Program (10041681, Development of fundamental technology for 10 nm process semiconductor and 10 G size large area process with high plasma density and VHF condition), funded by the Ministry of Knowledge Economy (MKE, Korea).

References and Notes

1. R. Brainard, G. Barclay, E. Anderson, and L. Ocola, *Microelec. Eng.* 62, 707 (**2002**).
2. J. Cobb, P. Dentinger, L. Hunter, D. O'Connell, G. Gallatin, B. Hinsberg, F. Houle, M. Sanchez, W. Domke, S. Wurm, U. Okoroyanwu, and S. H. Lee, *Proc. SPIE* 4688, 412 (**2002**).
3. J. P. Simons, D. L. Goldfarb, M. Angelopoulos, S. Messick, W. M. Moreau, C. Robinson, J. J. de Pablo, and P. F. Nealey, *Proc. SPIE* 4345, 19 (**2001**).
4. K. Hamamoto, T. Watanabe, H. Hada, H. Komano, and H. Kinoshita, *J. Photopolym. Sci. Technol.* 15, 361 (**2002**).
5. J. Cobb, R. Brainard, D. O'Connell, and P. Dentinger, *Mater. Res. Soc. Symp. Proc.* 705, 91 (**2002**).
6. M. Kakuchi, M. Hikita, and T. Tamamura, *Appl. Phys. Lett.* 48, 835 (**1986**).
7. H. T. Kim, B. S. Kwon, N. E. Lee, Y. S. Park, H. J. Cho, and B. Hong, *J. Vac. Sci. Technol., A* 26, 861 (**2008**).
8. S. J. Choi, *J. Vac. Sci. Technol., B* 25, 868 (**2007**).
9. K. Romero, R. Stephan, G. Grasshoff, M. Ruelke, K. Huy, J. Klais, S. Gowan, S. Bell, and M. Wright, *IEEE Trans. Semicond. Manuf.* 18, 539 (**2005**).
10. K. A. Pears, M. Stavrev, A. Scire, R. Koepe, M. Markert, U. Egger, and L. Donohue, *Microelectron. Eng.* 81, 156 (**2005**).
11. Y. S. Park, H. S. Myung, J. G. Han, and B. Y. Hong, *Thin Solid Films* 482, 275 (**2005**).
12. B. S. Kwon, J. S. Kim, H. K. Moon, and N. E. Lee, *Thin Solid Films* 518, 6451 (**2010**).
13. M. Pons, J. Pelletier, and O. Joubert, *J. Appl. Phys.* 75, 4709 (**1994**).
14. H. J. Lee, B. S. Kwon, Y. R. Park, J. H. Ahn, J. S. Kim, and N. E. Lee, *J. Kor. Phys. Soc.* 56, 1441 (**2010**).
15. O. V. Braginsky, A. S. Kovalev, D. V. Lopaev, E. M. Malykhin, T. V. Rakhimova, A. T. Rakhimov, A. N. Vasilieva, S. M. Zyryanov, K. N. Koshelev, V. M. Krivtsun, M. van Kaampen, and D. Glushkov, *J. Appl. Phys.* 111, 093304 (**2012**).
16. K. A. Pears, *Microelectron. Eng.* 77, 255 (**2005**).
17. H. J. Lee, B. S. Kwon, Y. R. Park, J. S. Kim, J. H. Ahn, J. W. Shon, and N. E. Lee, *Jpn. J. Appl. Phys.* 48, 8HD05 (**2009**).
18. S. Banna, A. Agarwal, K. Tokashiki, H. Cho, S. Rauf, V. Todorow, K. Ramaswamy, K. Collins, P. Stout, J. Y. Lee, J. Yoon, K. Shin, S. J. Choi, H. S. Cho, H. J. Kim, C. Lee, and D. Lymberopoulos, *IEEE Trans. Plasma Sci.* 37, 1730 (**2009**).
19. M. H. Jeon, A. K. Mishra, S.-K. Kang, K. N. Kim, I. J. Kim, S. B. Lee, T. H. Sin, and G. Y. Yeom, *Cur. Appl. Phys.* 13, 1830 (**2013**).
20. K. Tokashiki, et al., *Jpn. J. Appl. Phys.* 48, 08HD01 (**2009**).
21. S. Banna, A. Agarwal, G. Cunge, M. Darnon, E. Pargon, and O. Joubert, *J. Vac. Sci. Technol., A* 30, 040801 (**2012**).

Received: 17 August 2014. Accepted: 27 February 2015.